Accepted Manuscript

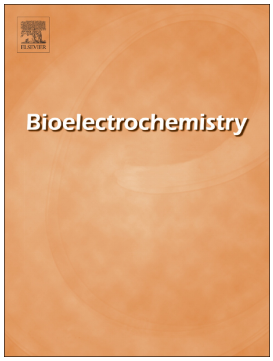

DNA biosensors based on gold nanoparticles-modified graphene oxide for the detection of breast cancer biomarkers for early diagnosis

Ayman Ali Saeed, Josep Lluís Acero Sánchez, Ciara K. O'Sullivan, Mohammed Nooredeen Abbas

PII: S1567-5394(17)30175-5
DOI: doi: 10.1016/j.bioelechem.2017.07.002
Reference: BIOJEC 7023

To appear in: *Bioelectrochemistry*

Received date: 22 March 2017
Revised date: 5 July 2017
Accepted date: 10 July 2017

Please cite this article as: Ayman Ali Saeed, Josep Lluís Acero Sánchez, Ciara K. O'Sullivan, Mohammed Nooredeen Abbas , DNA biosensors based on gold nanoparticles-modified graphene oxide for the detection of breast cancer biomarkers for early diagnosis, *Bioelectrochemistry* (2016), doi: 10.1016/j.bioelechem.2017.07.002

This is a PDF file of an unedited manuscript that has been accepted for publication. As a service to our customers we are providing this early version of the manuscript. The manuscript will undergo copyediting, typesetting, and review of the resulting proof before it is published in its final form. Please note that during the production process errors may be discovered which could affect the content, and all legal disclaimers that apply to the journal pertain.

ACCEPTED MANUSCRIPT

DNA biosensors based on gold nanoparticles-modified graphene oxide for the detection of breast cancer biomarkers for early diagnosis.

Ayman Ali Saeed[a], Josep Lluís Acero Sánchez[b], Ciara K. O'Sullivan[b,c*], Mohammed Nooredeen Abbas[a,*]

[a]*Electroanal. Lab., Applied Organic Chemistry Department, National Research Centre, El Bohouth St., Dokki, 12622 Giza, Egypt.*

[b]*Nanobiotechnology& Bioanalysis Group, Department of Chemical Engineering, Universitat Rovirai Virgili, 43007 Tarragona, Spain.*

[c]*Institució Catalana de Recerca I Estudis Avançats (ICREA), Passeig Lluís Companys 23, 08010 Barcelona, Spain*

Abstract

Two different DNA (ERBB2c and CD24c) modified gold nanoparticles and graphene oxide loaded on glassy carbon electrodes were prepared for early detection of breast cancer markers by electrochemical detection of HER2. Comparative study of ERBB2c and CD24c for the detection was carried out. A "sandwich-type" detection strategy was employed in this electrochemical DNA biosensor and its response was measured by amperometric detection. The electrochemical signal enhancement achieved via gold nanoparticles and grapheme oxide system allowed for sensitive detection of the breast cancer biomarker ERBB2 and the control marker CD24. The modified graphene oxide was characterised using Raman spectroscopy, UV-visible spectroscopy, Fourier transform infrared spectroscopy transmission electron microscopy, scanning electron microscopy and energy-dispersive X-ray spectroscopy. The various steps involved in the modification of a glassy carbon electrode with graphene oxide, gold nanoparticles and DNA probes, target and reporter probe were electrochemically characterised using cyclic voltammetry and electrochemical impedance spectroscopy. Using amperometric detection of a horse radish peroxidase label, detection limits of0.16nMand 0.23nMwere obtained with sensitivity 378 nA/nM and 219 nA/nM for ERBB2 andCD24 respectively.

Keywords: *DNA, Biosensor, Gold nanoparticles, Graphene Oxide, Breast Cancer, ERBB2 biomarker.*

Corresponding author:

ACCEPTED MANUSCRIPT

Mohammed Nooredeen Abbas, Email address: dr.nooreldin@yahoo.com

1. Introduction

Breast cancer is the most common cancer disease among women and it is the major cause of cancer mortality in females worldwide. Recent cancer statistics from the USA reported that around 29% of new cancer cases in females are breast cancer and approximately 14% of cancer mortality in females was caused by the breast cancer [1]. ERBB2 (also referred to as HER2, human epidermal growth factor receptor 2), is encoded by a proto-oncogene located at the long arm of human chromosome 17q, plays an important role in human malignancies and is over-expressed in a high number of human breast cancers [2,3]. Exosomes are endosome-derived nanovesicles actively released into the extracellular environment and biological fluids, both under physiological and pathological conditions, by different cell types. Extracellular vehicles (EVs) released by cancer cells can transfer mRNA, miRNA, and proteins to different recipient cells within the tumour microenvironment, in both an autocrine and Paracrine manner, causing a significant impact on signalling pathways, mRNA transcription, and protein expression [4]. The transfer of EVs to target cells, in turn, supports cancer growth, immunosuppression, and metastasis formation. The presence of HER2 on cancer cells is linked to increased cancer metastasis and tumour proliferation [5, 6]. Exosomes from SKBR3 and BT-474, both of which are HER2-overexpressing breast cancer cell lines, contain active HER2. The CD24, encoded by CD24 gene found on chromosome 6 (6q), is a small and heavily glycosylated cell surface protein which is frequently overexpressed in a wide range of carcinomas and is now considered as a prognostic marker in breast cancer [7, 8]. Several EV proteins are differentially expressed in certain stages and types of breast cancer and may be used as diagnostic markers of cancer progression or as a diagnostic marker, that is, “liquid biopsy” for general cancer diagnosis. For example, the oncogenic cancer marker CD24 [9] was uniquely expressed in serum-derived exosomes from breast cancer patients [10]. Recently, DNA biosensors have garnered increasing attention [11-14], being sensitive, inexpensive and simple diagnostic tools for genetic tests and can be miniaturized to satisfy point-of-care requirements. The use of these sensors allows the early diagnosis of cancer [13-15] as well as assisting in disease prognosis, facilitating a timely intervention with the appropriate therapy. DNA biosensors

ACCEPTED MANUSCRIPT

depend on sandwich hybridization assay have attracted much more attention of researchers [16,18]. The performance of DNA biosensors is highly dependent on the immobilisation of short capture DNA probes, complementary to the gene(s) to be interrogated, requiring optimal orientation and spacing for optimum target hybridisation. Reporter probe labelled with enzymes or redox molecules is also required to confirm the hybridization process between capture and target DNA. The incorporation of some advanced materials that have a high surface-to-volume ratio would allow the immobilization of much more capture probes that accordingly increase the sensitivity of the proposed sensor. Nanomaterials like carbon nanotubes [19, 20], graphene [21] and graphene oxide [22-24], gold nanoparticles [16, 25], silver nanoparticles [28], metal oxide nanomaterials [27] and quantum dots [28] offer stable and well-organized platforms for DNA immobilisation onto the sensor matrix that can markedly improve the sensor sensitivity. Graphene oxide (GO) is a carbon material with a two-dimensional organized carbon lattice, that contains functional groups like hydroxyl and carbonyl groups, which has attracted increasing interests for use in GO–DNA based sensors. Single-stranded DNA (ssDNA) can immobilise on GO through π–π stacking interaction [29]. While the function groups distributed in the GO surface provides a suitable anchor to covalently immobilize biomolecules through the formation of amide bonds with its amino groups [30, 31]. The efficiency of DNA immobilisation is further improved by incorporating metallic nanoparticles which possess excellent biocompatibility with biomolecules [32-34]. Decorating graphene oxide with metallic nanoparticles enhances its structural, electronic and catalytic properties [35, 36]. The covalent linkage of such nanoparticles onto GO sheet, increases the immobilisation opportunity toward the DNA analyte as they provide a higher surface area for its assembling on it, thus increasing the sensor sensitivity. Moreover, it is expected to improve the sensor durability. Thus, while the GCE modified directly with AuNPs may be used as a platform of DNA immobilization. However, the covalent immobilization of AuNPs to GO, not only allows for higher durability, but also enhances the electronic properties of each other resulting in enhanced sensitivity. The combination between sandwich-type system and nanoparticles that have a high surface-to-volume ratio would advantageously allow the immobilization of much more capture probes that accordingly increase the sensitivity of the proposed sensor. HER2 (human epidermal growth factor receptor 2) is one such gene that can play a role in the development of breast cancer. The HER2

ACCEPTED MANUSCRIPT

gene is also called the ERBB2 (Erb-B2 receptor tyrosine kinase 2) gene. The HER2 gene makes HER2 proteins. HER2 proteins are receptors on breast cells. Normally, HER2 receptors help control how a healthy breast cell grows, divides, and repairs itself. But in about 25% of breast cancers, the HER2 gene doesn't work correctly and makes too many copies of itself (known as HER2 gene amplification). All these extra HER2 genes tell breast cells to make too many HER2 receptors (HER2 protein overexpression). This makes breast cells grow and divide in an uncontrolled way. HER2 is a key prognostic marker and is a particularly important because HER2-positive cancers can be treated with targeted therapies. Normal individuals have HER2 levels in the range between 2 and 15 μg L^{-1} in blood [13]. The aim of the present work is the fabrication of an electrochemical DNA biosensor for early diagnosis of breast cancer by detection of its biomarkers (ERBB2 and CD24). The biosensor strategy is based on sandwich hybridization assay by immobilizing the capture DNA probe of the target DNA onto graphene oxide-modified gold nanoparticles. HRP-Labelled probe was then used to investigate the hybridization of capture probe and target DNA, and hence evaluate the concentration of the DNA biomarker in the sample.

2. Experimental

2.1. Materials

Potassium hexacyanoferrate(III) (>99%), potassium hexacyanoferrate(II) trihydrate (>99.99%), potassium chloride, sodium chloride, gold(III) chloride trihydrate (>99.9%), sodium citrate tribasic dihydrate, N-hydroxysuccinimide (NHS),N-(3-dimethylaminopropyl)-N’-ethylcarbodiimide hydrochloride(EDC), 4-aminothio-phenol, potassium permanganate, sulphuric acid, ethanol, sodium hydroxide, 6-mercaptohexanol, phosphate buffered saline pH 7.4, tris buffered saline pH 8.0, salmon sperm DNA (50 μg/mL) and Denhardt's solution were purchased from Sigma-Aldrich. Graphite powder was purchased from Riedel-de Haën. CD24, CD24-c, ERBB2, ERBB2-c and DNA-r (DNA-HRP) were obtained from biomers, and TMB one component HRP microwell substrate was from SurModics.

Capture probes (5'-3'):

ACCEPTED MANUSCRIPT

CD24: SH-TTTTTTTTTTTTTTTACATATACGAGCCTGTAGA

ERBB2: SH-TTTTTTTTTTTTTTTCTAGGAATTCGGCTACTTAG

Targets (5'-3'):

CD24:

GGGTTCCCTAAGGGTTGGACAAGTAACTCCTCCCAGAGTACTTCCAACTA
ATCCAACTAATGCCACCACCAAGGCGGCTGGTGGTGCCCTGCATCTACAG
GCTCGTATATGTATCTAGATTGGATCTTGCTGGCGCGTCC

ERBB2:

GGGTTCCCTAAGGGTTGGACGTTCTGAGGATTGTCAGAGCCTGACGCGCA
CTGTCTGTGCCGGTGGCTGTGCTAAGTAGCCGAATTCCTAGTCTAGATTGG
ATCTTGCTGGCGCGTCC

Reporter probe (5'-3'): HRP labelled probe – Complementary to all markers

HRP-5' TCCAACCCTTAGGGAACC 3'

2.2. Instrumentation and electrochemical procedures

The surface morphology and composition of the developed sensor were characterised using an environmental scanning electron microscopy (FEI ESEM Quanta 600 FEG) and energy dispersive X-ray spectroscopy (Oxford Instruments), respectively. Transmission electron microscope images were captured using (JEOL JEM-1011). Raman spectroscopy analysis was done by RENISHAW inVia Raman Microscope at 514 nm laser. UV-visible spectroscopy analysis was recorded by UV-2401PC. FTIR analysis was performed using JASCO FTIR spectrometer model 6100. The electrochemical experiments (cyclic voltammetry and electrochemical impedance spectroscopy) were performed using an electrochemical workstation model 660A CH Instruments Inc.The chronoamperometry analysis was done using an Autolab potentiostat/galvanostat (PGSTAT12) with a glassy carbon electrode (3 mm diameter) as the working electrode, while platinum wire and a standard Ag/AgCl electrode (filled with 3 M KCl) were used as the counter and reference electrodes, respectively.

2.3. Preparation of graphene oxide (GO)

ACCEPTED MANUSCRIPT

GO was prepared as per modified Hummers' method [37].10 g of graphite powder was added to 15mL solution of concentrated H_2SO_4, $K_2S_2O_8$ (5 g) and P_2O_5(5 g). After 6 h, the mixture was cooled to room temperature and then carefully diluted with Milli-Q water and finally filtered. The product was rigorously washed to remove the acid and then dried in air. 2 g of the dried product was added to 46 mL of cooled concentrated H_2SO_4 (0°C). Subsequently, 6 g$KMnO_4$ was added gradually under stirring conditions, at 35°C and stirred for 2 h. Milli-Q water (92 mL) was slowly added and the mixture was maintained for 15 min. The termination of the reaction was achieved by addition of Milli-Q water (280 mL) and 50 mL 30%H_2O_2. The product was filtered and washed with 500 mL 1:10 HCl solution. The obtained yellow-brown product was then washed with Milli-Q water and dried at room temperature.

2.4. Preparation of gold nanoparticles (AuNPs)

AuNPs were prepared as previously reported [38]. Briefly, 20 mg of gold(III) chloride trihydrate solution was added to 192 mL of Milli-Q water. The solution was heated until boiling. 8 mL of 1% (w/v) trisodium citrate was added rapidly under vigorous stirring conditions. The color changed from pale yellow to blue and finally red. The reaction solution was cooled to room temperature and stored at 4°C. The concentration of the prepared stock solution of gold nanoparticles was50 mg L^{-1}.

2*.5. Preparation of gold nanoparticles-modified graphene oxide (AuNPs-GO)*

AuNPs-GO was prepared as previously described, with some minor modifications [39-41]. The prepared graphene oxide (20mg) was suspended in 4 mL of absolute ethanol and sonicated for 1 h. EDC and NHS (0.05M) was added and mixed for 3 h. 10 mM of 4-aminothiophenol was added and the mixture stirred overnight. The obtained product was washed with ethanol 5 times and dried. 20 mg of the product was suspended in 100 mL of the prepared AuNPs solution and sonicated for 1 h followed by an overnight incubation at 4°C. The supernatant was removed and the obtained product was washed 5 times with Milli-Q water at room temperature then dried.

ACCEPTED MANUSCRIPT

2.6. Preparation of AuNPs-GO/GCE

Prior to electrochemical measurements, the glassy carbon electrode was polished with 1.0, 0.3, 0.05-micron size alumina powders, sonicated in ethanol and distilled water, washed with deionized water and dried using argon at room temperature. The AuNPs-GO (1mg) was suspended in 1 mL Milli-Q water and 5 µL was drop-casted onto the cleaned GCE and oven-dried at 50°C.A schematic diagram showing the prepared AuNPs-GO is presented in **Schematic 1**.

2.7. DNA sensor fabrication

To prepare the DNA sensor(CD24-c/AuNPs-GO/GCE), the thiol-terminated capture probe (CD24-c) was co-immobilized on the modified glassy carbon electrode (AuNPs-GO/GCE) with 6-mercaptohexanol (1:10). 8 µL of 100 µM CD24-c was mixed well with 72 µL of 100 µM 6-mercaptohexanol (prepared in 1 M KH_2PO_4), AuNPs-GO/GCE was then incubated in 25 µL of that mixture for 3 h under shaking conditions at 37°C. The sensor was immersed in Milli-Q water, stirred gently for 10 min and finally dried using argon at room temperature. The capture probe-modified sensor was incubated for 1 h in 25 µL of Denhardt's solution, diluted 1:20 with phosphate buffer (pH 7.4).

For the calibration curve measurements, the capture probe-modified electrode was incubated in25 µL of each concentration (20, 10, 6.6, 3.3, 1.1, 0.37 nM) of CD24 target, prepared in hybridization buffer (Tris buffer + 1 M NaCl, pH 8, 0.05 M), for 30 min at 37°Cunder shaking conditions. The sensor was then gently washed in Tris buffer (pH8, 0.05 M) and dried using argon gas. In the last step, the reporter DNA was hybridized with the target DNA by incubating the sensor in 25 µL of reporter probe (7 nM) for another 30 min. The sensor was again washed with Tris buffer and dried using argon gas. The same procedures were followed to prepare the ERBB2 sensor (ERBB2-c/AuNPs-GO/GCE). CD24 and ERBB2 targets were also determined by both sensors to evaluate the sensitivity of each sensor to its specific target.

3. Results and Discussion

ACCEPTED MANUSCRIPT

3.1. Non-electrochemical characterisations

3.1.1. UV-visible spectroscopy

The UV-Visible spectra of the prepared materials were recorded (**Fig.S1(A)**). The prepared AuNPs showed a characteristic absorption band at 524 nm. The absorption bands of GO at 231 and 305 nm were attributed to $\pi \rightarrow \pi^*$ transition of C=C and $n \rightarrow \pi^*$ transition of C=O bonds [42] and were due to the carbonyl groups of GO. The amide linkages formed between 4-aminothiophenol and GO decreased the band intensity of the free carbonyl groups of GO and a weak band appeared at 250 nm. The immobilisation of AuNPs was recognized by the disappearance of the gold peak at 524 nm due to covering of the surface of AuNPs [43].

3.1.2. FTIR

The recorded FTIR spectra showed a good indication for the success of the preparation process. As can be seen in **Fig.S1(B)**, graphite has no strong characteristic absorption peaks as it has no functional groups, only a peak at 3433 cm^{-1}, which is attributed to OH groups due to water hydration. GO shows a broad band at 3419 cm^{-1}(O-H stretch) starting from 1840 cm^{-1}, which together with the peaks at 1721 cm^{-1}(C=O stretch, carbonyl/carboxy), 1624 cm^{-1} (C=C stretch, aromatic), 1388 cm^{-1} (C-O, carboxy), 1212 (C-O stretch, epoxy) and 1050 cm^{-1} (C-O stretch, alkoxy) is indicative of the presence of graphene oxide as these bands are related to the skeleton of the graphene oxide [44-48]. The amide bond formation between GO and 4-aminothiophenol was identified by the appearance of an absorption band at 3216 cm^{-1}(N-H stretch) attributable to the presence of free secondary amine groups. The band at 3388 cm^{-1} proves that there were still some free carboxylic groups and the hydroxyl groups of the graphene oxide itself. The decrease in the band intensities following immobilisation on AuNPs is postulated to be due to an almost complete coverage of the gold.

3.1.3. Raman spectroscopy

ACCEPTED MANUSCRIPT

Raman spectroscopy is a non-destructive technique that is widely used to obtain structural information of carbon materials. Usually, the Raman spectrum of a GO film displays a D band at ~1350 cm^{-1} and a broad G band at ~1580 cm^{-1}[49]. The G band is characteristic of all sp^2-hybridized carbon networks, which originates from the first-order scattering from the doubly degenerate E_{2g} phonon modes of graphite in the Brillouin zone centre as well as bond stretching of sp^2 carbon pairs in both rings and chains. Meanwhile, the D band is due to the breathing mode of aromatic rings [50], which comes from the structural imperfections created by the attachment of oxygenated groups on the carbon basal plane [51]. Therefore, the D band intensity is often used as a measure for the degree of disorder [52]. Generally, the integrated intensity ratio of the D and G bands (I_D/I_G) indicates the oxidation degree and the size of sp^2 ring clusters in a sp^3/sp^2 hybrid network of carbon atoms. Another band around 2680 cm^{-1}, usually referred to as the 2D band, is the overtone of the D band, which reflects the number of graphene layers [53,54]. The 2D band is attributed to double resonance transitions resulting in production of two phonons with opposite momentum. In contrast to the D band, which is only Raman active in the presence of defects, the 2D band is active even in the absence of any defects [55]. Raman spectra of graphite, GO, ATP-GO and AuNPs-GO can be seen in **Fig. 1(A)**. The Raman spectra of graphite shows a band at 1572 cm^{-1} (sharp, G band) which are observed to be due to the graphitic carbonic sp^2 carbon atoms (C-C stretch) and at 1351 cm^{-1} (weak, D band) which is attributed to breathing of sp^2 carbon atoms [44,56,57]. The preparation of GO is accomplished by disorders in the sp^2-hybridized carbon sheets which was induced by the addition of oxygen during the oxidation process. These disorders resulted in an increase in the intensity of D band. The intensity ratio of the D and G bands (I_D/I_G) ratio increased once the graphene oxide had been prepared confirming the formation of large sp^3 domain [58]. The decrease of the 2D band at 2694 cm^{-1}indicates that the prepared graphene oxide has only a few layers [59].

3.1.4. SEM/EDS

A further demonstration of the success of the self-assembly of AuNPs on GO surface via the formation of Au-S bonds, was observed, with gold being identified as one of the surface components following surface modification(AuNPs-GO). As can be

ACCEPTED MANUSCRIPT

appreciated from **Fig. S2**, the SEM image of the AuNPs functionalised electrode exhibits a good distribution of AuNPs over the surface and EDS shows the presence of the gold signal.

3.1.5. TEM

TEM was recorded for AuNPs-GO to measure the diameter of AuNPs, to examine the distribution of the particles over GO, as well as confirming the success of the preparation steps. As can be observed in **Fig.1(B)**, AuNPs are well distributed and GO is decorated with AuNPs which are only found attached to GO and this indicates that the amide bond formation step (between GO and ATP) and the self-assembly (Au-S bond) were successfully achieved. The diameter of the particles was measured to be 13 nm.

3.2. Electrochemical characterisation (CV and EIS)

To characterize the modified electrode surface and confirm the success of each step of electrode modification, CV and EIS were recorded for the CD24 specific electrode after each step of modification in 5 mM $[Fe(CN)_6]^{3-/4-}$ (1:1) in 0.1 M KCl solution. As seen in **Fig.2(A)**, the electrodes were scanned from 0.7 to -0.2 V at a scan rate 100 mV/s and it is observed that each step of modification was accomplished by a change in the values of I_p and ΔE of the redox probe (**Table 1**) which is an indication for the surface modification. Nyquist plot is also recorded (**Fig. 2(B)**) at 0.2 V with a frequency range from 0.1 to 10^5 Hz. An equivalent electrical circuit was designed from the impedance spectrum, R_{ct} values (**Table 1**) were then calculated for each step of electrode modification. The change in the values of charge transfer resistance is another indication proving the modification and the hybridization process. The increase in R_{ct} value to 1062 Ω after drop-casting AuNPs-GO is attributed to the presence of GO which acts as an insulating layer that hindered electron transfer due to the disrupted sp2 bonding networks [16,60,61]. The immobilization of capture DNA probe and 6-mercaptohexanol also increased the R_{ct} value to 2017 Ωdue to the complete coverage of the gold nanoparticles and the negatively charged phosphate groups of the immobilized DNA probe which repeal the redox couple. The R_{ct} value increased again

ACCEPTED MANUSCRIPT

to 2630 Ω after the hybridization of the target DNA. While upon the addition of the reporter DNA probe the R_{ct} value increased to 4619 Ω, most probably due to the increase in the electrostatic repulsion as the phosphate groups increases after each step of hybridization and the steric hindrance caused by the hybridization and the introduction of HRP.

Table 1 The characteristic parameters of CV and EIS of the proposed sensor during different steps of its preparation

E. No	Surface composition	I_{Red} (µA)	I_{Ox} (µA)	ΔE (V)	R_{ct}(Ω)	C (µF)
1	Bare GCE	-71.13	70.52	0.109	141.6	0.413
2	AuNPs-GO/GCE	-49.69	45.46	0.192	1062	0.514
3	CD24-c/AuNPs-GO/GCE	-36.69	35.18	0.27	2017	0.490
4	CD24/CD24-c/AuNPs-GO/GCE	-34.62	28.71	0.309	2630	0.505
5	DNA-HRP/CD24/CD24-c/AuNPs-GO/GCE	-23.03	26.48	0.37	4619	0.445

3.3. Analytical performance

Once the capture probe (5'-3') is immobilized onto the modified electrode, its nitrogenous bases of 20 nucleotides will be available to hybridize with the complementary sequence of bases (3'-5') within the specific target DNA. Per this hybridization, another sequence of bases (3'-5') of the target DNA will hybridize with the HRP-labelled reporter probe (5'-3'). Reduced TMB (colourless) will be oxidized (blue) by HRP loaded on the reporter probe, equation 1.

$$TMB_{Red} + H_2O_2 \rightarrow TMB_{Oxi} + 2H_2O \qquad 1$$

Chronoamperometric measurements were fixed at -0.05V. This potential was chosen as it is negative enough to fully reduce the oxidized TMB.

3.3.1. Non-specific interactions

When cross-reactivity and specificity studies were carried out, with immobilised probes non-complementary to the target being interrogated e.g. ERBB2 probe and

ACCEPTED MANUSCRIPT

CD24 target, and vice-versa, a high non-specific current was observed, which was postulated to be due to adsorption of the HRP label onto the highly reactive GO and to address this a blocking step was introduced, and additionally the concentration of the labelled reporter probe was optimised (**Fig. 3A**).The CD24 specific and non-specific sensors (20 nM target was allowed to interact with both electrodes) were exposed to a range of concentrates of the HRP labelled reporter probe, with no appreciable difference between specific and non-specific observed at lower concentrations (0.4, 2 nM), but large differences observed at increasing concentrations, with the optimum concentration chosen to be 7nM. In addition, two blocking reagents were tested to decrease the non-specific binding (**Fig. 3B**); Denhardt's solution [62] diluted1:50 with phosphate buffer and salmon sperm DNA [63] at a concentration of 50 µg/mL. The salmon sperm DNA completely blocked the surface, to such an extent that the specific binding was also markedly decreased. The protein nature of the Denhardt's solution showed a good blocking function and a considerable decrease in the non-specific current was obtained, with the signal ratio between the CD24 specific electrode and non-specific electrode being 2.80 and 3.78 for the electrodes without and with Denhardt's solution, respectively. The concentration of the Denhardt's solution was also optimised, and the signal ratio between the CD24 specific and non-specific electrode was improved to6.18using a1:20 dilution of Denhardt's solution.

3.3.2. Calibration curves

The calibration curves were recorded using the optimised conditions of the chronoamperometric method. The calibration curve was plotted for two electrodes, one with an immobilisedCD24-c and the other with ERRB2-c. The surface was then blocked using Denhardt's solution (1:20) and the CD24 target was then introduced in different concentrations and finally 7 nM of DNA-HRP could hybridise with any bound target. The electrode was then immersed for 30 seconds in TMB and the current was recorded using chronoamperometry at -0.05V for 0.5 s (**Fig. S3**). As shown in **Fig.4A**, The CD24 specific electrode (CD24-c/AuNPs-GO/GCE) showed a linear current change when tested from 0.37 to 20 nM CD24and the CD24 non-specific electrode (ERBB2-c/AuNPs-GO/GCE) exhibited no current change over these concentrations, confirming the sensitivity and specificity of the CD24-c/AuNPs-

ACCEPTED MANUSCRIPT

GO/GCE. ERBB2 was also measured at different concentrations with the same electrodes and the same mentioned conditions (**Fig. 4B**), The ERBB2 specific electrode (ERBB2-c/AuNPs-GO/GCE) showed a current change with the different concentrations of ERBB2 while the ERRB2 non-specific (CD24-c/AuNPs-GO/GCE) showed no change. Finally, the current of the non-specific interactions was subtracted from that corresponding to the specific interaction to show the actual sensitivity (**Fig. 4C**) which is 219 and 378nA/nM for CD24 and ERBB2 targets, respectively. The detection limit was calculated to be 0.23 and 0.16nM for CD24 and ERBB2 specific electrodes respectively, based on signal to noise ratio = 3,(LOD = 3σ and σ = s (blank of specific signals) + s (blank of non-specific signals).The reproducibility was tested by recording the current of the same concentration of the target DNA three times with a fresh AuNPs-GO and DNA assay each time and the standard deviation of 0.37, 1.11, 3.33, 6.66, 10 and 20 nM of CD24 target was 0.053, 0.076, 0.18, 0.15, 0.14 and 0.16, respectively. The current of different concentrations of ERBB2 was also measured using the ERBB2 specific sensor, again three times for each concentration, and the standard deviation calculated for each concentration was 0.057, 0.070, 0.22, 0.096, 0.15, 0.086, respectively.

The regenerability was determined by repeating the current recorded fora selected concentration using the same sensor following exposure to 0.1 M NaOH. The regeneration removes the DNA target and the reporter probe so the immobilised capture probe was again available for a new assay. A concentration of 10 nM of the DNA was measured then the electrode was regenerated and measured again. The percentage current change observed was 4.6% and 2.0% for CD24 and ERBB2, respectively.

3.3.3. Comparison of some breast cancer biosensors

Table 2 summarizes a comparison with some other recent reports about breast cancer biosensors and illustrating the analytical benefits for using the proposed biosensor for the prognosis of the disease. Data in Ref. [15] describes an ultrasensitive electrochemical aptamer-based assay for detection of human epidermal growth factor receptor 2 protein (HER2) breast cancer biomarker. Results show that the reduced graphene oxide-chitosan (rGO-Chit) film as a suitable electrode material possesses

ACCEPTED MANUSCRIPT

great favourable properties including high homogeneity, good stability, large surface area and high fraction of amine groups as aptamer binding sites. Using methylene blue (MB) as an electrochemical probe and differential pulse voltammetry technique, two linear concentration ranges of 0.5–2 ng mL^{-1} and 2–75 ng mL^{-1} were obtained with a high sensitivity of 0.14 μA ng^{-1} ml and a very low detection limit of 0.21 ng mL^{-1} (very lower than the clinical cut-off). The fabricated aptasensor showed excellent selectivity for detection of HER2 in complex matrix of human serum samples. The sensitive detection of HER2 can be attributed to the multiple signal amplification of MB during its accumulation to the modified electrode surface via both affinity interaction to aptamer molecules and electrostatic adsorption to the HER2 analyte as well as high charge transfer kinetic properties of the applied rGO-Chit film. In Ref. [64] a sandwich type-based voltammetric sensor for HER2 was designed using an anti-HER2 antibody immobilized onto GNPs, modified with 2,5-bis(2-thienyl)-1H-pyrrole-1- (p-benzoic acid), and deposited on a GCE. A HER2-specific aptamer was conjugated with GNPs modified with hydrazine and used as a signalling probe. Following the immunoreaction, the sensor was immersed in a silver nitrate solution. Subsequently, the silver ions were reduced by hydrazine into silver metal and deposited onto the aptamer-GNPs conjugate. Using square wave stripping voltammetry (SWSV), the level of HER2 was determined over the range from 0.1 ng L^{-1} to 10 μg L^{-1}, with a LOD of 37 pg L^{-1}. Ref. [65] describes the fabrication of an immunosensor for HER2 using anti-HER2 antibody attached to iron oxide nanoparticles, which were deposited on a gold electrode surface. Using DPV, this sensor was shown to be responsive to HER2 concentrations over the linear ranges from 10 ng L^{-1} to 10 μg L^{-1} and 10 μg L^{-1} to 100 μg L^{-1}, with a LOD of 995 pg L^{-1}. In Ref. [66] a novel impedance aptasensor was developed by immobilizing HER2 (human epidermal growth factor receptor 2)-specific single stranded DNA aptamer onto the monolayer of 3-mercaptopropionic acid self-assembled on gold nanoparticles electrode. The efficiency of each electrode modification step and the performance of thus constructed aptasensor were assessed by impedance spectroscopy. The impedance response of the aptasensor showed a proportional relationship with the concentrations of HER2 ranged from 10^{-5} to 10^{2} ng mL^{-1}. The aptasensor showed fast HER2 detection with negligible cross reactivity to various compounds likely to exist in human serum samples (e.g. glucose, IgG, DNA and RNA), indicative of excellent sensitivity and specificity of the aptasensor. The aptasensor could be regenerated by a

ACCEPTED MANUSCRIPT

simple pH-shift method. Considering these advantages of the developed aptasensor, it could provide a good potential sensing platform for non-invasive early detection of breast cancer biomarker.

Table 2 Comparison of some breast cancer biosensors

Electrode material	**Technique**	**LR (nM)**	**LOD**	**Reference**
HER2/rGO/Chit	DPV	0.5–2 ng mL−1 & 2–75 ng mL−1	0.21ng mL^{-1}	15
GNPs / 2,5-bis(2-thienyl)-1H-pyrrole-1- (p-benzoic acid) /GCE	SWV	0.1ngL^{-1} -10.0 µg L^{-1}	37 pg L^{-1}	64
anti-HER2 antibody /iron oxide NPs / a gold electrode	DPV	10 ng L^{-1} to 10 µg L^{-1}	0.995 pg L^{-1}	65
HER2/3-mercaptopropionic acid/AuNPs	Impedimetry	10^{-5} to 10^{2} ng mL^{-1}		66
DNA-c/AuNPs-GO/GCE	CA	0.37-10 nM	0.16nM ERBB2 0.23nM CD24	This work

SWV: square wave voltammetry, DPV: Differential plus voltammetry, CA: Chronoamperometry

3.3.4. Analysis of spiked real sample

Sample from a cancer patient was collected and the Invisorb® Spin Tissue Mini Kit was used for its preparation for measurement. The sample was grinded under liquid nitrogen to increase the lysis efficiency. Lysis of the grinded sample was performed by incubating with 400 µL Lysis Buffer G and 40 µL Proteinase Kat 52°C. The sample was then centrifuged for 2 min at 11.000 rpm to spin down non-lysed material. The supernatant was transferred into a new 1.5 mL tube and 200 µL Binding Buffers A were added to the lysate which was then transferred onto an Invisorb® Spin Filter, placed into 2.0 mL receiver tube and incubated for 1 min at room temperature. The genomic DNA was adsorbed onto the membrane as the lysate was drawn through by centrifugal force for 3 min at 12.000 rpm and the filtrate was discarded. A 550 µL

ACCEPTED MANUSCRIPT

Wash Buffer was added onto Spin Filter and centrifuged for 1 min at 11.000 rpm to remove remaining contaminants and enzyme inhibitors then the filtrate was discarded. The washing was repeated once more. The genomic DNA was eluted from the spin filter by incubating with200 µL pre-warmed Elution Buffer at room temperature for 3 min. Centrifugation for 1 min at 11.000 rpm was applied and the spin filter was discarded. Finally, the eluate contains ready to use DNA. This DNA was used as a biological matrix to spike some concentrations of ERBB2 and CD24 targets. 5 µL of 10 and 20 nM of ERBB2 were mixed well with 20 µL of the extracted DNA sample to prepare 2 and 4 nM of ERBB2.

Table 3 Determination of the ERBB2 DNA breast cancer biomarker in spiked real sample

Sample	Added, nM	Found, nM	SD, ± nM (n=3)	RSD, %	Recovery, %
Spiked real sample	0	ND	-	-	-
	2.00	2.58	0.07	2.86	129
	4.00	4.17	0.26	6.39	104

*ND: Not detectable

4. Conclusions

Gold nanoparticle-modified graphene oxide (AuNPs-GO) grafted on GCE has been proved to be an excellent platform for the immobilisation of thiolated nucleic acid capture probes. The electrochemical detection of the breast cancer marker ERBB2 and the control marker CD24 using this platform showed clearly the signal enhancement achieved via AuNPs and GO. Using amperometric detection of a horse radish peroxidase label as reporter probe, detection limits of 1.6×10^{-10} M and 2.3×10^{-10}M were obtained with sensitivity 378 nA/nM and 219nA/nM for the target ERBB2 and CD24, respectively. As, the normal level of ERBB2 (HER2) in blood is 2-15 µg L^{-1}, thus our developed sensor can be used safely for the early stage screening of breast cancer.

ACCEPTED MANUSCRIPT

Acknowledgements

The authors wish to thank and acknowledge EU for supporting this work through FP7 Marie Curie IRSES Project: Micro/nano sensors for early cancer warning system – diagnostic and prognostic information "SMARTCANCERSENS". The authors would like also to acknowledge Prof. Dr. Wafaa Hassan El-Metnawy, Director of GENOME ONCO CENTER, Professor of Cancer Radiation Biology and Ex-Chairman of Oncology Department, School of Medicine, Cairo University for supporting us with a real sample.

References

[1] R.L. Siegel, K.D. Miller, A. Jemal, Cancer statistics, 2016, A Cancer Journal for Clinicians 66 (2016) 7-30.

[2] S. Tsutsui, S. Ohno, S. Murakami, Y. Hachitanda, S. Oda, Prognostic value of c-erbB2 expression in breast cancer, J. Surg. Oncol. 79 (2002) 216-223.

[3] J.S. Ross, J.A. Fletcher, The HER-2/neu Oncogene in Breast Cancer: Prognostic Factor, Predictive Factor, and Target for Therapy, *Oncologist* 3 (1998) 237-252.

[4] T. M. Green, M. L. Alpaugh, S. H. Barsky, G. Rappa, A. Lorico, Breast Cancer-Derived Extracellular Vesicles: Characterization and Contribution to the Metastatic Phenotype, *BioMed Research International* Volume 2015, Article ID 634865, 13 pages

[5] Y. M. Li, Y. Pan, Y. Wei et al., Upregulation of CXCR4 is essential for HER2-mediated tumour metastasis, *Cancer Cell* 6 (2004) 459–469.

[6] W. Dean-Colomb and F. J. Esteva, HER2-positive breast cancer: Herceptin and beyond, *European Journal of Cancer* 44, (2008) 2806–2812.

[7] G. Kristiansen, K.-J. Winzer, E. Mayordomo, J. Bellach, K. Schlüns, C. Denkert, E. Dahl, C. Pilarsky, P. Altevogt, H. Guski, M. Dietel, CD24 expression is a new prognostic marker in breast cancer, *Clin. Cancer Res.* 9 (2003) 4906-4913.

[8] P. Athanassiadou, D. Graspa, M. Gonidi, A.M. Athanassiadou, A. Tsipis, E. Patsouris, CD24 expression has a prognostic impact in breast carcinoma, *Pathology Res. Prac*. 205 (2009) 524-533

ACCEPTED MANUSCRIPT

[9] X. Fang, P. Zheng, J. Tang, and Y. Liu, CD24: from A to Z," *Cellular and Molecular Immunology*, 7 (2010) 100–103.

[10] A.K. Rupp, C. Rupp, S. Keller et al., Loss of EpCAM expression in breast cancer derived serum exosomes: role of proteolytic cleavage, *Gynecologic Oncology* 122 (2011) 437–446.

[11] A. Benvidi, A.D. Firouzabadi, M.D. Tezerjani, S.M. Moshtaghiun, M. Mazloum-Ardakani, A. Ansarin, A highly sensitive and selective electrochemical DNA biosensor to diagnose breast cancer, *J. Electroanal. Chem.* 750 (2015) 57–64.

[12] O.Y.F. Henry, J.L.A. Sanchez, C.K. O'Sullivan, Bipodal PEGylated alkanethiol for the enhanced electrochemical detection of genetic markers involved in breast cancer, *Biosens. Bioelectron.* 26 (2010) 1500–1506.

[13] M. Hasanzadeh , N. Shadjou, M. de la Guardia, "Early stage screening of breast cancer using electrochemical biomarker detection" Trends in Analytical Chemistry 91 (2017) 67-76

[14] L. Chun, S. Kim, M. Cho, W. Choe, J. Nam, D. W. Lee, Y. Lee, "Electrochemical detection of HER2 using single stranded DNA aptamer modified gold nanoparticles electrode", Sensors and Actuators B 186 (2013) 446– 450

[15] A. Tabasi, A. Noorbakhsh, E. Sharifi, "Reduced graphene oxide-chitosan-aptamer interface as new platform for ultrasensitive detection of human epidermal growth factor receptor 2" Biosensors and Bioelectronics 95 (2017) 117–123

[16] A.-L. Liu, G.-X. Zhong, J.-Y. Chen, S.-H. Weng, H.-N. Huang, W. Chen, L.-Q. Lin, Y. Lei, F.-H. Fu, Z.-L. Sun, X.-H. Lin, J.-H. Lin, S.-Y. Yang, A sandwich-type DNA biosensor based on electrochemical co-reduction synthesis of graphene-three-dimensional nanostructure gold nanocomposite films, *Anal. Chim. Acta* 767 (2013) 50–58.

[17] J. Wang, A. Shi, X. Fang, X. Han, Y. Zhang, An ultrasensitive super sandwich electrochemical DNA biosensor based on gold nanoparticles decorated reduced graphene oxide, *Anal. Biochem.* 469 (2015) 71–75.

[18] J. Mandli, H. Mohammadi, A. Amine, Electrochemical DNA sandwich biosensor based on enzyme amplified microRNA-21 detection and gold nanoparticles, *Bioelectrochem.* 116 (2017) 17–23.

[19] J.E. Weber, S. Pillai, M.K. Ram, A. Kumar, S.R. Singh, Electrochemical impedance-based DNA sensor using a modified single walled carbon nanotube electrode, *Mater. Sci. Eng.* C 31 (2011) 821–825.

ACCEPTED MANUSCRIPT

[20] X. Tang, S. Bansaruntip, N. Nakayama, E. Yenilmez, Y. Chang, Q. Wang, Carbon Nanotube DNA Sensor and Sensing Mechanism, *Nano Lett.* 6 (2006) 1632–1636.

[21] P.A. Rasheed, N. Sandhyarani, Graphene-DNA electrochemical sensor for the sensitive detection ofBRCA1 gene, *Sens. Actuat. B* 204 (2014) 777–782.

[22] A. Benvidi, A.D. Firouzabadi, S.M. Moshtaghiun, M. Mazloum-Ardakani, M.D. Tezerjani, Ultrasensitive DNA sensor based on gold nanoparticles/reduced graphene oxide/glassy carbon electrode, *Anal. Biochem*. 484 (2015) 24–30.

[23] L. Gao, C. Lian, Y. Zhou, L. Yan, Q. Li, C. Zhang, L. Chen, K. Chen, Graphene oxide-DNA based sensors, *Biosens. Bioelectron.* 60 (2014) 22–29.

[24] B. Li, G. Pan, N.D. Avent, R.B. Lowry, T.E. Madgett, P.L. Waines, Graphene electrode modified with electrochemically reduced graphene oxide for label-free DNA detection, *Biosens. Bioelectron*. 72 (2015) 313–319.

[25] M.T. Castañeda, S. Alegret, A. Merkoçi, Electrochemical Sensing of DNA Using Gold Nanoparticles, *Electroanal.* 19 (2007) 743–753.

[26] H. Li, Z. Sun, W. Zhong, N. Hao, D. Xu, H.-Y. Chen, Ultrasensitive Electrochemical Detection for DNA Arrays Based on Silver Nanoparticle Aggregates, *Anal. Chem.* 82 (2010) 5477–5483.

[27] M. Chen, C. Hou, D. Huo, M. Yang, H. Fa, An ultrasensitive electrochemical DNA biosensor based on a copper oxide nanowires/single-walled carbon nanotubes nanocomposite, *Appl. Surf. Sci.* 364 (2016) 703–709.

[28] X. Fuku, B. Singh, R.F. Ajayi, A.N. Jijana, P. Baker, E. Dempsey, E. Iwuoha, A gallium telluride quantum dots bioelectrode system for human epidermal growth factorreceptor-2 (HER2/neu) oncogene signaling, *Anal. Meth.* 7 (2015) 6114-6124.

[29] Z.W. Tang, H. Wu, J.R. Cort, G.W. Buchko, Y.Y. Zhang, Y.Y. Shao, I.A. Aksay, J. Liu, Y.H. Lin, Constraint of DNA on Functionalized Graphene Improves its Biostability and Specificity, *Small* 6 (2010) 1205–1209.

[30] Y. Wang, Z. Li, J. Wang, J. Li, Y. Lin, Graphene and graphene oxide: biofunctionalization and applications in biotechnology, *Biotech.* 29 (2011) 205-212.

[31] D. Sharma, S. Kanchi, M.I. Sabela, K. Bisetty, Insight into the biosensing of graphene oxide: Present and future prospects, *Arab. J. Chem.* 9 (2016) 238-261.

[32] K. Saha, S.S. Agasti, C. Kim, X. Li, V.M. Rotello, Gold Nanoparticles in Chemical and Biological Sensing, *Chem. Rev.* 112 (2012) 2739-2779.

ACCEPTED MANUSCRIPT

[33] S. Zeng, K.-T. Yong, I. Roy, X.-Q. Dinh, X. Yu, F. Luan, A Review on Functionalized Gold Nanoparticles for Biosensing Applications, *Plasmonics* 6 (2011) 491-506.

[34] J.M. Pingarrón, P. Yáñez-Sedeño, A. González-Cortés, Gold nanoparticle-based electrochemical biosensors, *Electrochim. Acta* 53 (2008) 5848-5866.

[35] Y.Z. Zhang, W. Jiang, Decorating graphene sheets with gold nanoparticles for the detection of sequence-specific DNA, Electrochim. Acta 71 (2012) 239–245.

[36] L. Gao, C. Lian, Y. Zhou, L. Yan, Q. Li, C. Zhang, L. Chen, K. Chen, Graphene Oxide-DNA Based Sensors, Biosens. Bioelectron. 60 (2014) 22-29.

[37] Y.J. Zhang, M. Geng, H. Zhang, Y. He, C. Peng, Q. Huang, C.H. Fan, High-conductivity graphene nanocomposite via facile, covalent linkage of gold nanoparticles to graphene oxide, Chinese Sci. Bull. 57 (2012) 3086.

[38] M.N. Abbas, A.A. Saeed, B. Singh, A.A. Radowan, E. Dempsey, A cysteine sensor based on a gold nanoparticle-iron phthalocyanine modified graphite paste electrode, Anal. Meth. 7 (2015) 2529.

[39] J.M. You, D. Kim, S.K. Kim, M.-S. Kim, H.S. Han, S. Jeon, Novel determination of hydrogen peroxide by electrochemically reduced graphene oxide grafted with aminothiophenol-Pd nanoparticles, Sens. Actuat. B 178 (2013) 450.

[40] M.L. Yola, N. Atar, Z. Üstündağ, A.O. Solak, A novel voltammetric sensor based on p-aminothiophenol functionalized graphene oxide/gold nanoparticles for determining quercetin in the presence of ascorbic acid, J. Electroanal. Chem. 698 (2013) 9.

[41] T.A. Pham, B.C. Choi, K.T. Lim, Y.T. Jeong, A simple approach for immobilization of gold nanoparticles on graphene oxide sheets by covalent bonding, Appl. Surf. Sci. 257 (2011) 3350–3357.

[42] J. Chen, B. Yao, C. Li, G. Shi, An improved Hummers method for eco-friendly synthesis of graphene oxide, Carbon 64 (2013) 225-229.

[43] M. Kesik, F.E. Kanik, G. Hızalan, D. Kozanoglu, E.N. Esenturk, S. Timur, L. Toppare, A functional immobilisation matrix based on a conducting polymer and functionalized gold nanoparticles: Synthesis and its application as an amperometric glucose biosensor, Polymer 54 (2013) 4463-4471.

[44] D.C. Marcano, D.V. Kosynkin, J.M. Berlin, A. Sinitskii, Z. Sun, A. Slesarev, L.B. Alemany, W. Lu, J.M. Tour, Improved Synthesis of Graphene Oxide, ACS Nano 4 (2010) 4806-4814.

ACCEPTED MANUSCRIPT

[45] X. Yang, L. Ma, S. Wang, Y. Li, Y. Tu, X. Zhu, Clicking graphite oxide sheets with well-defined polystyrenes: A new Strategy to control the layer thickness, Polymer 52 (2011) 3046–3052.

[46] C. Hontoria-Lucas, A.J. López-Peinado, J.de D. López-González, M.L. Rojas-Cervantes, R.M. Martín-Aranda, Study of oxygen-containing groups in a series of graphite oxides: Physical and chemical characterization, Carbon 33 (1995) 1585–1592.

[47] S.Y. Toh, K.S. Loh, S.K. Kamarudin, W.R.W. Daud, Graphene production via electrochemical reduction of graphene oxide: Synthesis and characterization, Chem. Eng. J. 251 (2014) 422-434.

[48] W.J. Kim, C. Basavaraja, P.X. Thinh, D.S. Huh, Structural characterisation and DC conductivity of honeycomb-patterned poly(ε-caprolactone)/gold nanoparticle-reduced graphite oxide composite films, Mater. Lett. 90 (2013) 14-18.

[49] A.K. Agegnehu, C.-J. Pan, J. Rick, J.-F. Lee, W.-N. Su, B.-J. Hwang, Enhanced hydrogen generation by cocatalytic Ni and NiO nanoparticles loaded on graphene oxide sheet, J. Mater. Chem. 22 (2012) 13849-13854.

[50] F. Tuinstra, J.L. Koeing, Raman Spectrum of Graphite, J. Phys.Chem. 53 (1970) 1126–1130.

[51] J. Zhang, J. Yu, M. Jaroniec, J.R. Gong, Noble metal-free reduced graphene oxide-ZnxCd$_1$ -xS nanocomposite with enhanced solar photocatalytic H_2 -production performance, Nano Lett. 12 (2012) 4584–4589.

[52] J. Yang, X. Zeng, L. Chen, W. Yuan, Photocatalytic water splitting to hydrogen production of reduced graphene oxide/SiC under visible light, Appl. Phys. Lett. 102 (2013) 083101–083104.

[53] P.D. Tran, S.K. Batabyal, S.S. Pramana, J. Barber, L.H. Wong, S.C. Loo, A cuprous oxide-reduced graphene oxide (Cu2O-rGO) composite photocatalyst for hydrogen generation: employing rGO as an electron acceptor to enhance the photocatalytic activity and stability of Cu2O, Nanoscale 4 (2012) 3875-3878.

[54] A. Mukherji, B. Seger, G.Q. Lu, L. Wang, Nitrogen doped Sr2Ta2O7 coupled with graphene sheets as photocatalysts for increased photocatalytic hydrogen production, ACS Nano 5 (2011) 3483-3492.

ACCEPTED MANUSCRIPT

[55] J. Hou, Z. Wang, W. Kan, S. Jiao, H. Zhu, R.V. Kumar, Efficient visible-light-driven photocatalytic hydrogen production using CdS@TaON core–shell composites coupled with graphene oxide nanosheets, J. Mater. Chem. 22 (2012) 7291–7299.

[56] K. Dave, K.H. Park, M.Dhayal, Two-step process for programmable removal ofoxygen functionalities of graphene oxidefunctional, structural and electrical characteristics, *RSC Adv.* 5 (2015) 95657-95665.

[57] S. Stankovich, D.A. Dikin, R.D. Piner, K.A. Kohlhaas, A. Kleinhammes, Y. Jia, Y. Wu, S.T. Nguyen, R.S. Ruof, Synthesis of graphene-based nanosheets via chemical reduction of exfoliated graphite oxide, *Carbon* 45 (2007) 1558–1565.

[58] V. Singh, D. Joung, L. Zhai, S. Das, S.I. Khondaker, S. Seal, Graphene based materials: past, present and future, *Prog. Mater. Sci*. 56 (2011) 1178-1271.

[59] P. Wang, Z.-G. Liu, X. Chen, F.-L. Meng, J.-H. Liu, X.-J. Huang, UV irradiation synthesis of an Au-graphene nanocomposite with enhanced electrochemical sensing properties, *J. Mater. Chem*. A 1 (2013) 9189-9195.

[60] D.R. Dreyer, S. Park, C.W. Bielawski, R.S. Ruoff, The chemistry of graphene oxide, *Chemical Society Reviews* 39 (2010) 228–240.

[61] Y. Hu, F. Li, X. Bai, D. Li, S. Hua, K. Wang, L. Niu, Label-free electrochemical impedance sensing of DNA hybridization based on functionalized graphene sheets, *Chem. Comm.* 47 (2011) 1743–1745.

[62] H. Berney, J. West, E. Haefele, J. Alderman, W. Lane, J.K. Collins, A DNA diagnostic biosensor: development, characterization and performance, *Sens. Actuat. B* 68 (2000) 100-108.

[63] M. Svobodova, T. Mairal, P. Nadal, M.C. Bermudo, C.K. O'Sullivan, Ultrasensitive aptamer based detection of β-conglutin food allergen, *Food Chem.* 165 (2014) 419–423.

[64] Y. Zhu, P. Chandra, Y.-B. Shim, Ultrasensitive and selective electrochemical diagnosis of breast cancer based on a hydrazine-Au nanoparticle-aptamer bioconjugate, Anal. Chem. 85 (2013) 1058-1064.

[65] M. Emami, M. Shamsipur, R. Saber, R. Irajirad, An electrochemical immunosensor for detection of a breast cancer biomarker based on antiHER2-iron oxide nanoparticle bioconjugates, Analyst 139 (2014) 2858-2866

ACCEPTED MANUSCRIPT

[66] L. Chun, S. Kim, M. Cho, W. Choe, J. Nam, D. W. Lee, Y. Lee, Electrochemical detection of HER2 using single stranded DNA aptamer modified gold nanoparticles electrode, Sens. Actuat. B 186 (2013) 446– 450

ACCEPTED MANUSCRIPT

ACCEPTED MANUSCRIPT

Figures captions:

Schematic 1, Schematic presentation of the proposed sandwich-type DNA sensor, the prepared AuNPs-GO/GCE showing the hybridization of target DNA with the specific capture probe and HRP-labelled probe.

Fig. 1 (A) Raman spectra of the prepared materials at 520nm for 20s. **(B)** TEM of (a) GO and (b) AuNPs-GO.

Fig. 2 (A) CV from 0.7 to -0.2 Vat 100 mV/s and **(B)** EIS from 0.1 to 10^5 Hz at 0.2 V for CD24 specific electrode in 5 mM$[Fe(CN)_6]^{3-/4-}$ for (a)■ bare GCE, (b) AuNPs-GO/GCE, (c) ▲CD24-c/AuNPs-GO/GCE, (d) ♦ CD24/CD24-c/AuNPs-GO/GCE and (e) ∗ DNA-HRP/CD24/CD24-c/AuNPs-GO/GCE.

Fig. 3 (A) Optimization of the concentration of DNA-HRP (20 nM target DNA) for CD24 specific (blue) and CD24 non-specific (red). **(B)** Testing of Denhardt's solution (1:50 and 1:20) and Salmon sperm DNA as blocking reagents (20 nM CD24) for CD24 specific (blue) and CD24 non-specific (red).

Fig. 4 Calibration curves of **(A)** CD24 target at (●) specific and (●) non-specific electrodes and **(B)** ERBB2 target at (♦) specific and (♦) non-specific electrodes. **(C)** The calibration curve of (●) CD24 and (♦) ERBB2 targets representing the specific current only.

ACCEPTED MANUSCRIPT

ACCEPTED MANUSCRIPT

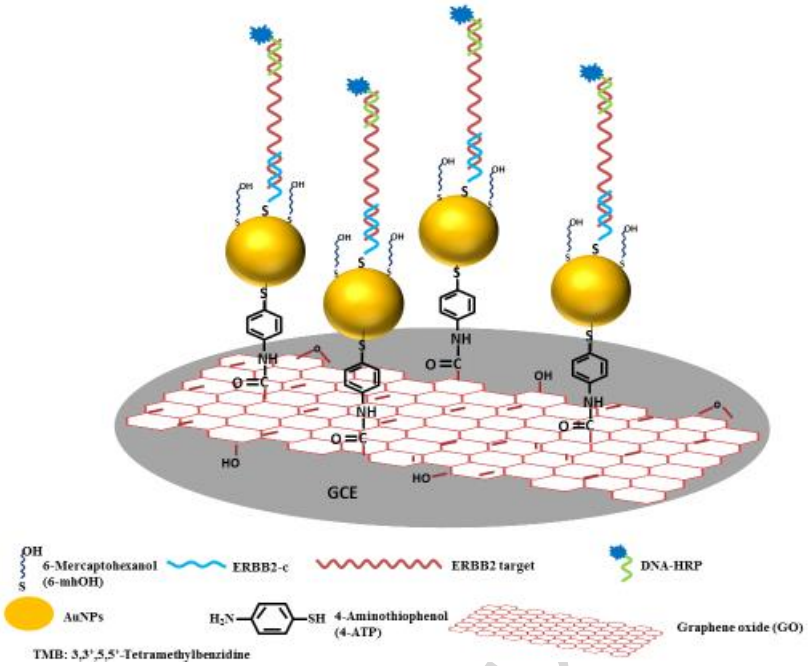

Schematic 1

ACCEPTED MANUSCRIPT

ACCEPTED MANUSCRIPT

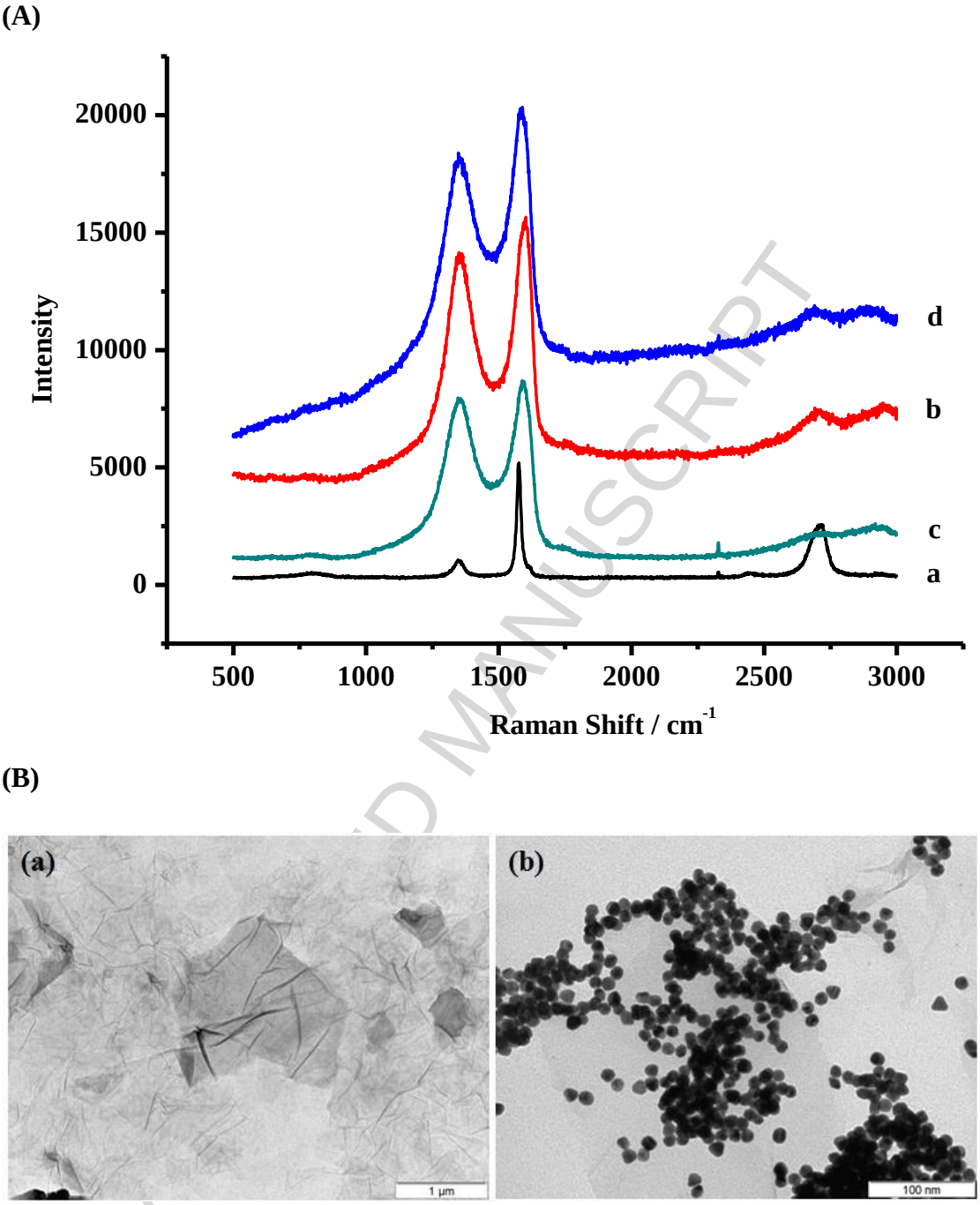

Fig. 1

ACCEPTED MANUSCRIPT

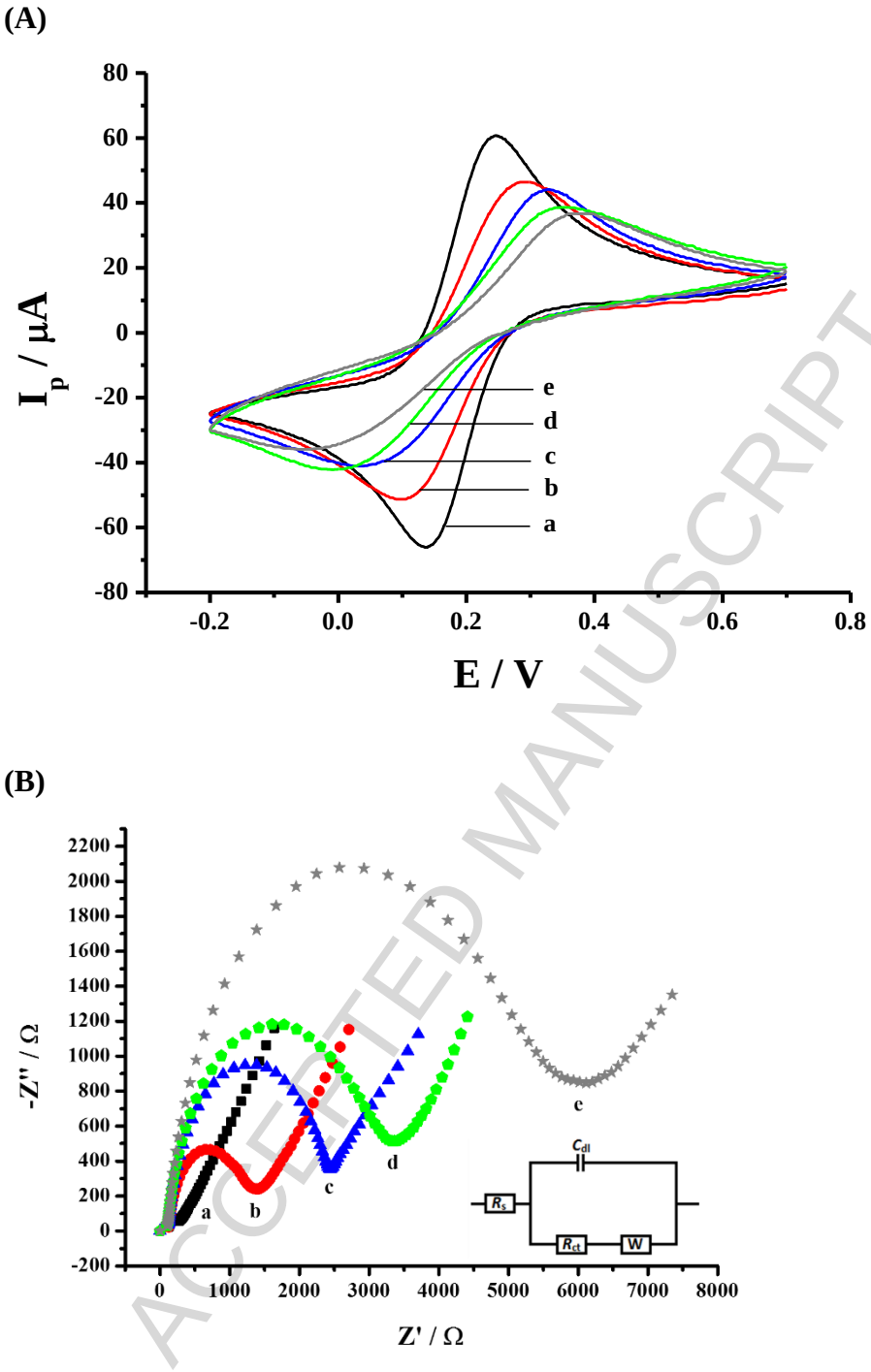

Fig. 2

ACCEPTED MANUSCRIPT

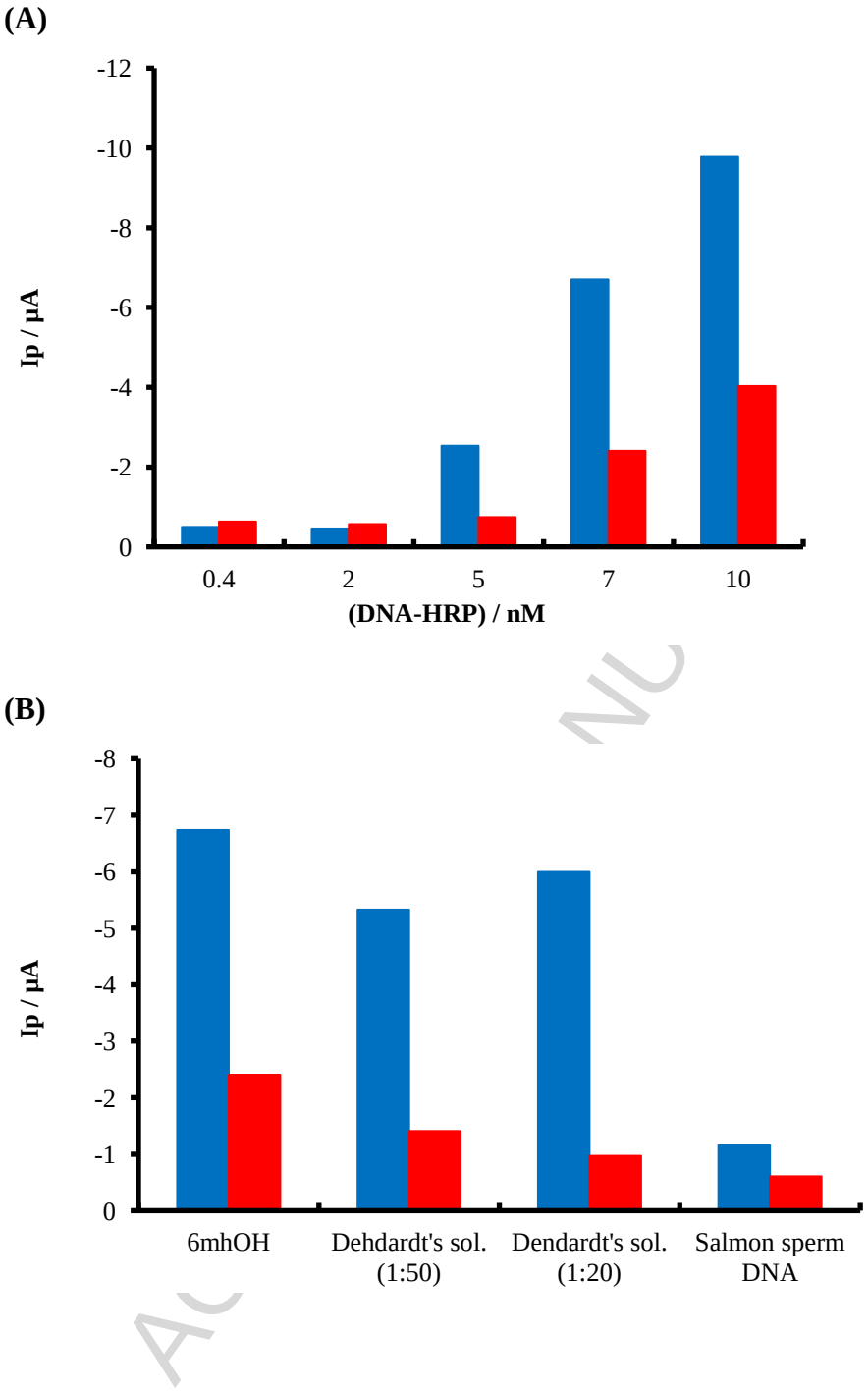

Fig. 3

ACCEPTED MANUSCRIPT

(A)

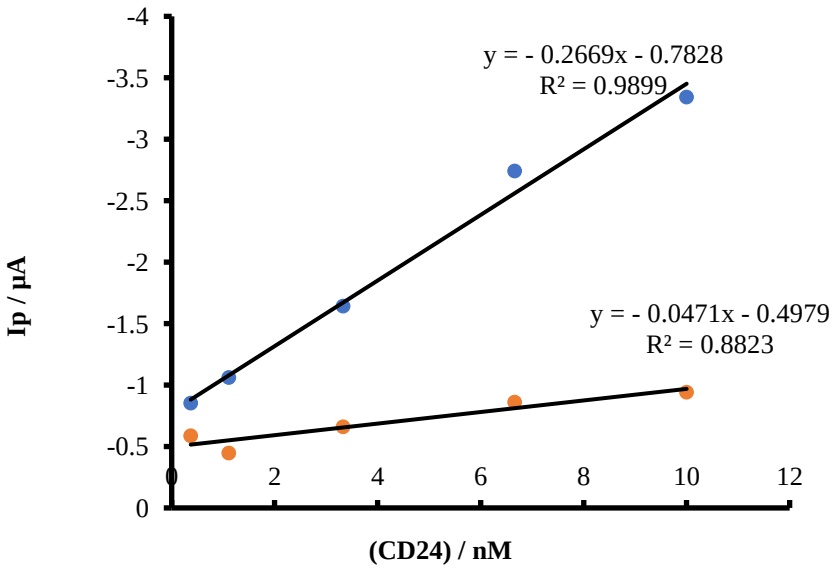

ACCEPTED MANUSCRIPT

ACCEPTED MANUSCRIPT

(B)

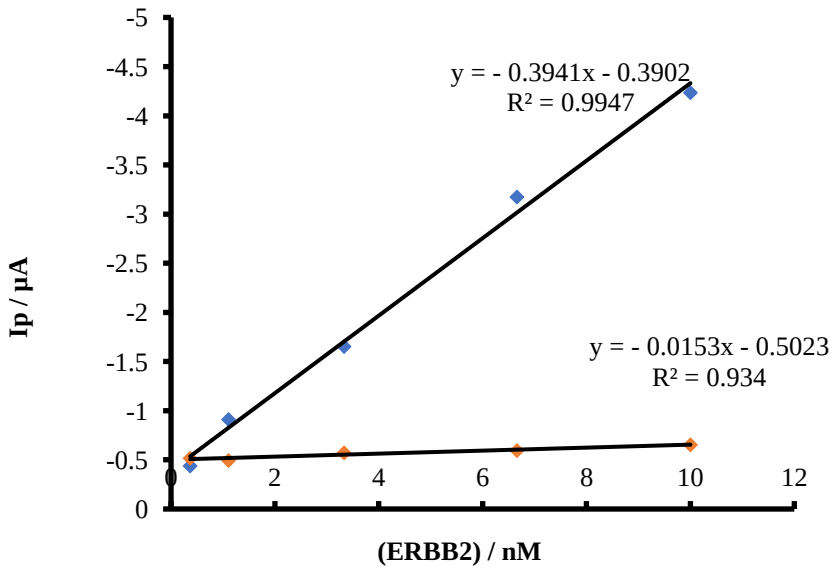

ACCEPTED MANUSCRIPT

ACCEPTED MANUSCRIPT

(C)

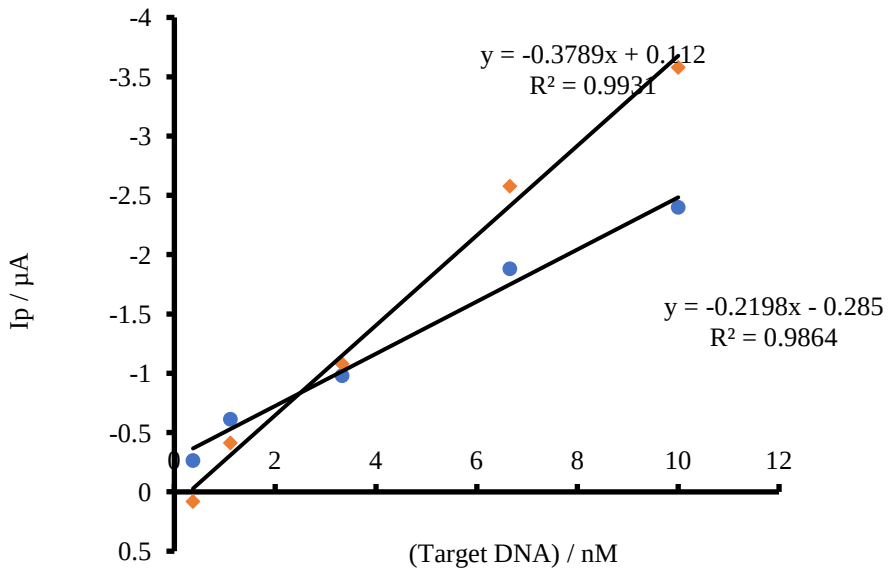

Fig. 4

ACCEPTED MANUSCRIPT

ACCEPTED MANUSCRIPT

Highlights:

-Gold nanoparticles were linked to graphene oxide and then grafted on to glassy carbon.

-Thiolated nucleic acid capture probes were surface immobilised.

-The signal enhancement achieved allowed sensitive detection of breast cancer marker ERBB2

-The control marker CD24 was also detected at low concentration

ACCEPTED MANUSCRIPT